

# Theory of polarization enhancement in epitaxial BaTiO<sub>3</sub>/SrTiO<sub>3</sub> superlattices

J. B. Neaton and K. M. Rabe

Department of Physics and Astronomy, Rutgers University,  
Piscataway, New Jersey 08855-0849

(November 6, 2018)

The spontaneous polarization of epitaxial BaTiO<sub>3</sub>/SrTiO<sub>3</sub> superlattices is studied as a function of composition using first-principles density functional theory within the local density approximation. With the in-plane lattice parameter fixed to that of bulk SrTiO<sub>3</sub>, the computed superlattice polarization is enhanced above that of bulk BaTiO<sub>3</sub> for superlattices with BaTiO<sub>3</sub> fraction larger than 40%. In contrast to their bulk paraelectric character, the SrTiO<sub>3</sub> layers are found to be *tetragonal and polar*, possessing nearly the same polarization as the BaTiO<sub>3</sub> layers. General electrostatic arguments elucidate the origin of the polarization in the SrTiO<sub>3</sub> layers, with important implications for other ferroelectric nanostructures.

PACS: 64.70.Nd, 68.65.Cd, 77.22.Ej, 77.84.Dy

Experimental capabilities now allow layer-by-layer epitaxial growth of perovskite-based oxides, facilitating the exploration of a wide range of artificial materials inaccessible by conventional solid-state synthesis. Recently, short-period BaTiO<sub>3</sub>/SrTiO<sub>3</sub> superlattices, with modulation lengths down to three perovskite layers, have been grown on SrTiO<sub>3</sub> substrates using pulsed-laser deposition (PLD)<sup>1</sup> and reactive molecular beam epitaxy (MBE).<sup>2</sup> These superlattices are reportedly free of dislocations and coherently matched to the substrate, implying misfit strains of over 2% in the BaTiO<sub>3</sub> layers. Strains of this magnitude are expected to increase the polarization,<sup>3,4</sup> and the superlattice geometry preserves the high-strain state and prevents relaxation of the BaTiO<sub>3</sub> (BT) layers. But since the BT layers are interleaved with SrTiO<sub>3</sub> (ST), which has zero spontaneous polarization in the bulk, the degree to which the overall polarization might be enhanced in the superlattice remains in question.

In this Letter, we address this issue directly through study of a series of ideal short-period BT/ST superlattices with varying composition using first-principles density functional calculations. Our calculations show that these superlattices are ferroelectric, and predict that some possess polarizations significantly larger than bulk BT. An atomic-level analysis also reveals a significant *non-zero polarization* and strain in the ST layers, a direct result of internal polarizing fields originating in the BT layers. These results, consistent with recent measurements,<sup>1,2</sup> illustrate the importance of electrical boundary conditions for sustaining polarization in these and other nanoscale ferroelectric materials.

To predict the ground state structure and polarization in BT/ST superlattices with various numbers of BT layers, we use density functional theory within the local density approximation (LDA).<sup>5</sup> A plane-wave basis set and projector-augmented wave potentials<sup>6</sup> as implemented in the Vienna *ab initio* Simulations Package (VASP)<sup>7,8</sup> are employed. We consider period-five superlattices epitaxially grown on ST, and construct 1×1×5 supercells, designated 4/1, 3/2, 2/3, and 1/4, where the notation  $x/y$  refers to  $x$  perovskite layers of BT and  $y$  layers of ST.

The underlying ST substrate is treated implicitly by constraining the in-plane lattice constant of each superlattice to 3.863 Å, the value we calculate for the equilibrium lattice constant of cubic ST. The computed in-plane lattice constant for bulk tetragonal BT (3.945 Å) is likewise slightly smaller than experiment, a well-known artifact of the LDA. The resulting mismatch between the theoretical lattice constants is 2.1%, in excellent agreement with that observed experimentally. The ions within each supercell are allowed to relax toward equilibrium along [001], within space group  $P4mm$  (point group  $C_{4v}$ ), until the Hellmann-Feynman forces are less than 10<sup>-3</sup> eV/Å; the total energy with respect to the normal (or  $c$ -axis) lattice parameter of each superlattice is minimized concurrently. Brillouin zone (BZ) integrations are performed with a 6×6×2 Monkhorst-Pack mesh. A 44 Ry plane-wave cutoff is used for all calculations. For Berry-phase polarizations,<sup>9</sup> we find that 6  $k$ -points/string along [001] and 6 strings in the irreducible wedge provide well-converged results.

All calculations are performed under periodic, “short-circuit” boundary conditions, equivalent to a metallic substrate with the lattice constant of ST and full charge compensation on top and bottom “electrode” layers. Canting of polarization toward [111] is found to be energetically unfavorable, although we defer to a future study a full investigation of the possibility of zone-boundary octahedral rotations, such as those present in ST at low temperature.<sup>10,11</sup>

The  $c/a$  lattice parameters computed for the four period-5 superlattices, as well as those for bulk ST (0/5) and bulk strained BT (5/0), are provided in Table I. With the in-plane lattice parameter fixed to the computed ST lattice constant, the  $c/a$  ratio of BT expands to 1.0685 (×5 layers = 5.3426 for the 5/0 superlattice), in agreement with the experimentally determined Poisson ratio,<sup>1,2</sup> and the  $c/a$  ratio and cell volume decrease by about 2% per additional SrTiO<sub>3</sub> layer. The decrease in  $c/a$  results in a concomitant reduction in the polar distortion within each layer. This is quantified by dividing each superlattice into five Ti-centered unit cells (or

TABLE I. Structural parameters computed for superlattices with in-plane lattice constant  $a = 3.863 \text{ \AA}$ , and with  $l_{\text{ST}}$  layers of  $\text{SrTiO}_3$  and  $l_{\text{BT}}$  layers of  $\text{BaTiO}_3$  ( $\alpha$  is their ratio).  $\langle c/a \rangle_{\text{BT}}, \langle c/a \rangle_{\text{ST}}$ , and  $\langle c/a \rangle_{\text{I}}$  are the average local  $c/a$  parameters within BT, ST, and interface layers for each superlattice, as described in the text.  $P_0 = 24.97 \text{ \mu C/cm}^2$  is the computed value for bulk tetragonal  $\text{BaTiO}_3$ . Blank entries indicate layers absent for a given  $\alpha$ .

$l_{\text{BT}}/l_{\text{ST}}$	$\alpha$	$c/a$	$\langle c/a \rangle_{\text{BT}}$	$\langle c/a \rangle_{\text{ST}}$	$\langle c/a \rangle_{\text{I}}$	$P/P_0$
5/0	0	5.3426	1.0685			1.570
4/1	0.25	5.2502	1.0609		1.0338	1.435
3/2	0.667	5.1820	1.0566	1.0077	1.0306	1.249
2/3	1.5	5.1181	1.0526	1.0055	1.0272	1.000
1/4	4	5.0510		1.0018	1.0227	0.520
0/5	$\infty$	5.0000		1.0000		0.000

layers), with A cations at the corners, and examining local displacements from the pseudocubic positions within each layer. The individual perovskite layers are labeled as BT, if bounded by two BaO layers; ST, if bounded by SrO layers; or I, if bounded by one BaO and one SrO layer (one of the two interface layers within the supercell). The distance between neighboring A cations can be regarded as a local  $c/a$ ; the average values of this ratio for each layer type,  $\langle c/a \rangle$ , appear Table I. The large  $\langle c/a \rangle_{\text{BT}}$  are expected, based on the considerable in-plane strain.<sup>4</sup> More surprisingly, the average local  $c/a$  of the ST layers deviates slightly from unity: the ST unit cell is evidently *expanded* within the superlattice relative to the bulk. The strain is accompanied by relative displacements within the ST layers, where in particular we find the equatorial oxygens (Wyckoff positions 2c) to move significantly offsite.

The observed structural trends are reflected in the computed superlattice polarizations, also given in Table I. Despite the presence of one SrO layer, the polarization of the 4/1 superlattice is predicted to be considerably enhanced over that of BT under standard conditions in the bulk, and also larger than expected if the ST were nonpolar. Replacing one BaO layer with SrO reduces the polarization by only about 10%, while a simple scaling of the polarization by the volume fraction of BT would result in a 20% reduction. The 3/2 and 2/3 superlattices are found to retain 80 and 64% of the polarization of pure strained BT, again surpassing the scaled values of 60% and 40%. The simple scaling argument is inadequate because it assumes bulk behavior for the ST and strained BT layers, and neglects any electrostatic coupling between them. Internal polarizing fields play an essential role in determining the properties of these superlattices, as has been noted previously for other superlattice systems.<sup>12,13</sup>

To gain insight into the electrostatic coupling between layers, we decompose the total superlattice polarization into contributions from the individual Ti-centered perovskite layers defined above. (An alternate but equally

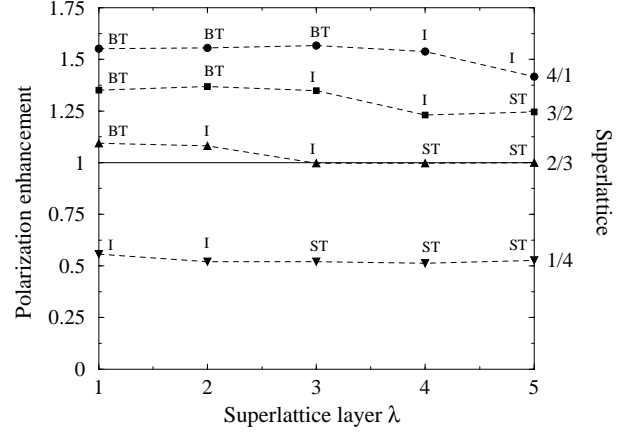


FIG. 1. Local polarization enhancement ( $P_\lambda/P_0$ ) by layer  $\lambda$  for each superlattice. Each layer is labeled BT, ST, or I as discussed in the text. As before,  $P_0 = 24.97 \text{ \mu C/cm}^2$ .

valid A cation-centered local cell choice does not result in significant changes in our analysis.) The local polarization  $P_\lambda$  of cell  $\lambda$  is expressed as a function of displacements within that cell as

$$P_\lambda \cong \sum_i \frac{\partial P}{\partial u_{\lambda 0i}} (u_{\lambda i} - u_{\lambda 0i}) = \frac{1}{\Omega} \sum_i Z_i^* \Delta u_{\lambda i}, \quad (1)$$

where  $\Delta u_{\lambda i}$  is the displacement of ion  $i$  in unit cell  $\lambda$ ,  $Z_i^*$  is the dynamical effective charge of ion  $i$ , and  $\Omega$  is the volume of the superlattice supercell. (All polarizations and displacements are along [001].) Since there are two different apical O ions (corresponding to Wyckoff positions 1b) associated with the buckled AO plans bounding the cell, we average their contribution to each cell, i.e.,  $\Delta \bar{u}_{\lambda,1b} = \frac{1}{2}(\Delta u_{\lambda+1,1b} + \Delta u_{\lambda,1b})$ . A similar prescription has previously been used in a study of domain walls in  $\text{PbTiO}_3$ .<sup>14</sup> The dynamical effective charges are evaluated by finite differences, in a reference structure with atomic displacements identically zero within every layer; their values will appear elsewhere.<sup>15</sup>

In Figure 1 the local polarization is shown as a function of layer for each superlattice. The most conspicuous feature of these profiles that the local polarization is nearly *constant* throughout each superlattice, minimizing electrostatic energy costs associated with the build-up of polarization charge  $\nabla \cdot \mathbf{P}$  at the interfaces. Not only are the ST layers polarized, but their local polarizations are close to those of the BT layers. Notably, the ST polarization, induced by the presence of the BT layers, is significant even in the 1/4 superlattice with just a single BaO layer, and even in the absence of in-plane strain. The polarization in the BT layers, on the other hand, is reduced and close in magnitude to that in the ST layers. If the local polarizations of the BT and ST layers were taken as those of the bulk, then the electric fields within the constituent BT and ST layers would be finite and have opposite signs. The field within the BT layers

would oppose the polarization, and that in the ST layers would polarize the nominally nonpolar layers.

To examine this in more detail, we model the system by two slabs of linear dielectric media, having dielectric constants  $\epsilon_b$  and  $\epsilon_s$ , in a parallel plate geometry. Short-circuit boundary conditions require the electric fields within each slab to be related by  $\mathcal{E}_b l_{BT} = -\mathcal{E}_s l_{ST}$ , where  $l_{BT}$  and  $l_{ST}$  correspond to the number of layers of BT and ST, as in Table I. Setting their electric displacements  $D = \mathcal{E} + 4\pi P$  to be equal, and using  $P_s = \chi_s \mathcal{E}_s$  and  $P_b = \chi_b \mathcal{E}_b + P_{5/0}$ , the polarization of each of the two slabs can be expressed in terms of the dielectric constants of the two materials, the initial spontaneous polarization,  $P_{5/0}$ , of strained BT, and their respective thicknesses. The average of the total slab polarization  $\bar{P}$ , weighted by the number of layers of each constituent, then becomes

$$\bar{P} = \frac{P_{5/0}}{1 + \alpha(\epsilon_b/\epsilon_s)}, \quad (2)$$

where  $\alpha = l_{ST}/l_{BT}$  and  $P_{5/0}$  is the computed polarization of strained BT, here  $39.20 \mu\text{C}/\text{cm}^2$  (as in Table I). This macroscopic formula, valid to linear order in the dielectric constants, can be seen to explain the composition dependence of the superlattice polarization. In Fig. 2 we plot the total polarization of each superlattice, calculated from first principles, against  $\alpha$ . We then perform a one-parameter fit to this data, obtaining the dashed curve in Fig. 2. Notice that the curve approximates the data remarkably well, even though our expression for the polarization is derived from macroscopic electrostatics and the superlattice layers are atomically thin. Thus to maximize the superlattice polarization, one must increase the fraction of BT layers (while preserving the high strain state), consistent with the recent measurements of Shimuta *et al.*<sup>1</sup> It is particularly striking that even for superlattices containing as little as 40% BT, one can expect to achieve a polarization as large as that of bulk BT.

The novel properties of short-period superlattice materials are, quite generally, expected to arise from three separate effects. The first is the sustainability of large strains in sufficiently thin lattice-mismatched layers. This can produce a significant change in properties from the bulk at standard conditions, manifest here in the enhanced polarization of the BT layers. We also expect electrostatic effects if the two materials have different susceptibilities or a *polarization mismatch* (i.e., different bulk polarizations), as in the present case. Indeed, internal fields can largely determine polarization and structural properties, resulting in a uniform polarization throughout this chemically inhomogeneous BT/ST system. Finally, we anticipate changes in properties associated with a high concentration of interfaces, where the bonding and structure will in general depart from that of the interior of the layers or the bulk. While in this system the interfaces are relatively gentle, apparently playing a minor role in the structure and polarization, they may be important or even dominant in other superlattice structures, espe-

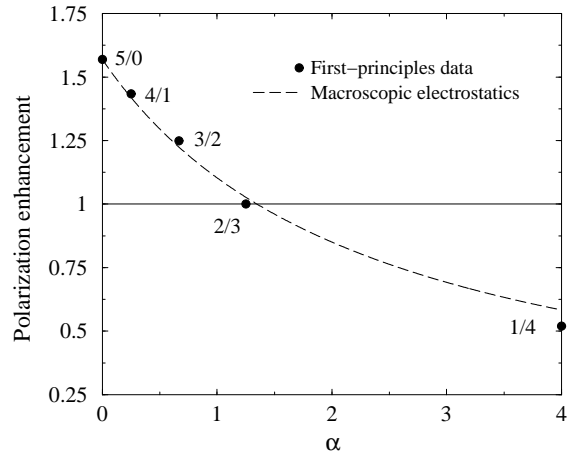


FIG. 2. Polarization enhancement ( $\bar{P}/P_0$ ), computed from first principles, as a function of  $\alpha = l_s/l_b$  for each superlattice (filled circles).  $\epsilon_b/\epsilon_s=0.4229$  provides the best fit of our calculations to Eq. (2).

cially if the thickness of the individual constituent layers is only a few unit cells.

In conclusion, we have shown, using a series of first-principles calculations, that significant polarization enhancement can be achieved in perovskite oxide superlattices. This enhancement arises from the combined effects of strain, induced in the BT layers by the epitaxial growth, and internal electric fields, associated with the superlattice geometry, which polarize the ST layers. The induced polarization observed here complements a previous prediction of ferroelectricity in ST layers under epitaxial stress.<sup>3,16</sup> Our analysis reveals important physical factors that influence the behavior of the superlattice system for given constituent layers and thickness, which will aid in the prediction of properties of a wider class of systems and provide a valuable guide for the design of artificially-structured materials.

## ACKNOWLEDGMENTS

We thank C. H. Ahn, M. H. Cohen, X. Q. Pan, D. G. Schlom, and D. Vanderbilt for valuable discussions. This work was supported by NSF-NIRT DMR-0103354 and ONR N00014-00-1-0261.

<sup>1</sup> T. Shimuta, O. Nakagawara, T. Makino, S. Arai, H. Tabata, and T. Kawai, *J. Appl. Phys.* **91**, 2290 (2002).

<sup>2</sup> W. Tian, X. Q. Pan, J. H. Haeni, and D. G. Schlom (unpublished).

- <sup>3</sup> N. A. Pertsev, A. G. Zembligotov, and A. K. Tagantsev, Phys. Rev. Lett. **80**, 1988 (1998).
- <sup>4</sup> J. B. Neaton, C.-L. Hsueh, and K. M. Rabe, Mat. Res. Soc. Sym. Proc. **718**, 311 (2002).
- <sup>5</sup> P. Hohenberg and W. Kohn, Phys. Rev. **136**, 864B (1964); W. Kohn and L. J. Sham, Phys. Rev. **140**, 1133A (1965).
- <sup>6</sup> P. Blöchl, Phys. Rev. B **50**, 17953 (1994); G. Kresse and D. Joubert, Phys. Rev. B **59**, 1758 (1999).
- <sup>7</sup> G. Kresse and J. Hafner, Phys. Rev. B **47**, R558 (1993).
- <sup>8</sup> G. Kresse and J. Furthmüller, Phys. Rev. B **54**, 11169 (1996).
- <sup>9</sup> D. King-Smith and D. Vanderbilt, Phys. Rev. B. **47**, 1651 (1993).
- <sup>10</sup> P. A. Fleury, J. F. Scott, and J. M. Worlock, Phys. Rev. Lett. **21**, 16 (1968).
- <sup>11</sup> N. Sai and D. Vanderbilt, Phys. Rev. B **62**, 13942 (2000).
- <sup>12</sup> J. Shen and Y. Ma, Phys. Rev. B **61**, 14279 (2000).
- <sup>13</sup> M. Sepiarsky, S. R. Phillpot, D. Wolf, M. G. Stachiotti, and R. L. Migoni, Phys. Rev. B **64**, 060101 (2001).
- <sup>14</sup> B. Meyer and D. Vanderbilt, Phys. Rev. B **65**, 104111 (2002).
- <sup>15</sup> J. B. Neaton and K. M. Rabe (unpublished).
- <sup>16</sup> N. A. Pertsev, A. K. Tagantsev, and N. Setter, Phys. Rev. B **61**, R825 (2000).